Elastic Actuation for Legged Locomotion

Chongjing Cao[1 2 a)] and Andrew Conn[1 2]
[1]Department of Mechanical Engineering, University of Bristol,
Queen's Building, University Walk, Bristol, BS8 1TR
[2]Bristol Robotics Laboratory
Bristol, BS16 1QY

ABSTRACT

The inherent elasticity of dielectric elastomer actuators (DEAs) gives this technology great potential in energy efficient locomotion applications. In this work, a modular double cone DEA is developed with reduced manufacturing and maintenance time costs. This actuator can lift 45 g of mass (5 times its own weight) while producing a stroke of 10.4 mm (23.6% its height). The contribution of the elastic energy stored in antagonistic DEA membranes to the mechanical work output is experimentally investigated by adding delay into the DEA driving voltage. Increasing the delay time in actuation voltage and hence reducing the duty cycle is found to increase the amount of elastic energy being recovered but an upper limit is also noticed. The DEA is then applied to a three-segment leg that is able to move up and down by 17.9 mm (9% its initial height), which demonstrates the feasibility of utilizing this DEA design in legged locomotion.

Keywords: dielectric elastomer actuators, elastic energy recovery, legged locomotion

[a)] Corresponding author: cc15716@bristol.ac.uk

1. INTRODUCTION

Dielectric elastomer actuators (DEAs) are an emerging actuation technology that have advantages over conventional actuators with regards to their large active strains, high energy density, scalability and low cost [1]. By taking advantage of the DEA film contraction in thickness and extension in area when actuated, a variety of possible actuation configurations can be designed to meet the desired shape and output degrees of freedom (DOF). To increase the maximum stroke, negative springs, or bistable elements are often seen in DEA designs. For example, [2] utilized rubber bands as an off-the-centre mechanism in a diamond DEA and achieved over 100% stroke. Based on the same concept, [3] achieved a 170% stroke on a single cone DEA. In nature, groups of muscles are typically configured to work antagonistically to perform multi-DOF movements. Taking inspiration from this, many multi-DOF DEAs have been developed: [4] produced a spring roll design with two DOF and a 5 DOF cone DEA is proposed by [5] and [6], which can be extended this into a 6 DOF elastic cube actuator [7].

In recent years, several legged robots actuated by different DEAs have been developed. FLEX1 [8] is known as the first DEA driven legged robot, with bowtie DEAs used in this robot. Later in FLEX 2, rolled DEAs replaced the bowtie DEA and demonstrated a higher efficiency and faster response. In [4], a six leg walking robot (MERbot) was developed using the spring roll DEAs with 2-DOF on each leg. [9] produced a biomimetic quadruped robot driven by multi-stacked DEAs. In 2015, the same research group proposed a hexapod robot driven by 3-DOF cone actuators capable of performing an alternating tripod gait [10]. [11] showed an micro hopping leg using cone DEA with a bi-stable spring.

In Nature, it is very common that animals take advantage of elastic elements to save energy in locomotion, for example, horses have been found to be able to save up to 40% of the mechanical work at a slow trot due to their elastic tendons [12]. In this work we propose a double cone DEA design with novel modular assembly that is dynamically tested to analyze the

energy transition and elastic energy recovery of the actuator. To demonstrate the feasibility of using this actuator in energy efficient legged locomotion, we apply this actuator to drive a bespoke three-segment leg prototype.

2. MODULAR DOUBLE CONE DEA DESIGN

This double cone DEA design, as applied by [5] and [6], consists of two single DE membranes stretched over a rigid rod in the center which maintains the tension. The two single conical DEA membranes can be actuated separately to produce bidirectional actuation. To achieve a multi-layer DEA of such configuration, a common procedure is to stack two DEA layers directly with one layer of compliant electrode sandwiched in between. This layout can cause two issues: (i). the failure of one layer of DEA membrane in this multi-layered stack would require the whole DEA assembly to be replaced, which can be time and cost expensive; (ii). the stroke output of a multi-layer DEA is usually less than that of a single layer one, which could be due to the interaction of the compliant electrodes sandwiched between two neighbouring layers.

Based on the above limitations, a modular double cone configuration is proposed. In this design, mating surfaces at either end of the central rod are avoided by incorporating acrylic dome caps to reduce the stress concentration near the edge. Each layer of DEA membrane is bonded to a different outer frame, and is separated from other layers by a small gap, thus different layers will not directly interface. Figure 1 illustrates a CAD model of this design. With this modular design, even if one layer of DEA fails, it can be easily removed and replaced. Also for an actuator with *N* layers DEA membranes, it could, in theory, output the same stroke as a single membrane cone DEA but with *N* times the force.

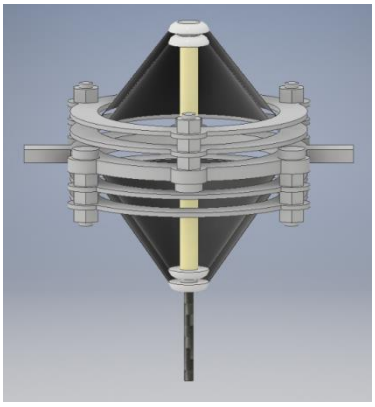

Figure 1. CAD model of a modular double cone DEA design.

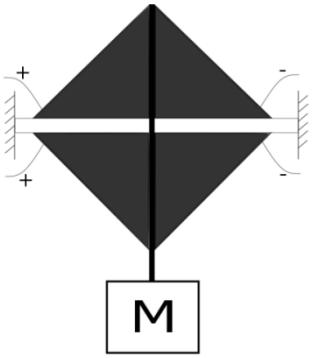

Figure 2. Double cone DEA and mass system.

3. EXPERIMENTS

To investigate the energy recovery of a double cone DEA in legged robot applications, we first introduce a DEA-mass system, as illustrated in Figure 2. This model can be viewed as a simplified actuator-spring-mass leg model commonly used in legged locomotion analysis. By analyzing the energy transfer in this model, we are able to predict the feasibility of utilizing a double cone DEA in legged locomotion for both actuation and elastic energy storage.

In this work, VHB 4905 (3M) is chosen for its large electro-active area strain and high energy density as well as commercial availability. A general fabrication process of this double cone DEA is described as follows. First, two pieces of VHB 4905 tape are biaxially pre-stretched 4×4 and then bonded to outer frames which are laser cut from 1 mm thick acrylic sheet. Acrylic dome caps with 9 mm diameter and 2 mm height are centrally aligned and bonded on the underside of each membrane. Carbon conductive grease (M.G. Chemicals Ltd) is adopted as the compliant electrodes and copper tape is used as a connection between compliant electrodes and high voltage cables. Outer frames are fixed to a central frame by nylon fasteners. One 40 mm height nylon spacer is used in the center to maintain the tension on the DEA membranes. A 2mm

diameter carbon fiber rod is fixed to one dome cap and passes outwards through the hollow spacer and the opposite dome cap until it protrudes out of the actuator. Any load can be connected to the actuator through this carbon fiber rod.

3.1 Energy transfer in DEA-mass system

In this experiment, four types of energy changes will be measured, which are the gravitational potential energy, $E_{Gpotential}$, and kinetic energy, $E_{kinetic}$, of the load and the moving parts of the DEA, elastic potential energy of the DEA, $E_{elastic}$, and the electrical energy input $E_{electrical\text{-}in}$, as defined in Equations (1-4):

$$E_{Gpotential}(t) = (M+m)gh(t) \quad , \tag{1}$$

$$E_{kinetic}(t) = \frac{1}{2}(M+m)V^2(t) \quad , \tag{2}$$

$$E_{electrical-in}(t) = \int_{t_0}^{t} U(t)i(t)dt \quad , \tag{3}$$

$$E_{elastic}(t) = \int_{0}^{h(t)} Fdh \quad , \tag{4}$$

where t is the time (s), M is the mass of the load, m is the mass (kg) of the parts on DEA that move with the load (the mass of DEA membranes is considered negligible), $h(t)$ is the displacement (m) of the load relative to the mounted frame of DEA, $V(t)$ is the velocity of the load (m/s), $U(t)$ is the voltage across the DEA (V), $i(t)$ is the current flow from high voltage amplifier into the DEA (A) and F is the elastic force of the DEA as a spring (N).

It should be noted that the elastic energy considered in the presented analysis is not the total elastic energy stored in DEA membranes but rather the net energy stored by the DEA as a spring where the rest position (no load, no driving voltage) is the zero energy point, i.e. pre-stretch and central spacer induced elastic potential energy in manufacturing is neglected. The passive reaction force on the DEA against displacement can be modelled based on the geometry of the DEA and strain energy function (SEF) (see [13] for example), but in this work we apply an experimental approach to directly measure the reaction force of the DEA as a function of displacement. The experimental method is described as follows. The outer frame of the DEA was fixed to a testing rig while leaving the central spacer free to move. A set of 10 g weights were incrementally added to a plate connecting to the DEA's carbon fiber rod and the corresponding displacement was recorded by laser displacement sensor (LK-G152 and LKGD500, Keyence). Due to the stress relaxation effect of the DEA material, both stretch and roil weight against displacements were recorded.

Voltage across the top and bottom cone DEAs and current flows were measured with the build-in voltage and current monitor units of the high voltage amplifiers (Ultravolt 5HVA23-BP1) used in this experiment. The height h is measured by a laser sensor placed above the centre of DEA. The velocity is the derivative of the height by time.

A 45 g mass is attached to the rod of the actuator, as shown in Figure 3(a). An alternating square driving voltage (3kV amplitude) is applied to the top and bottom cone DEA membranes thus moving the load up and down, as shown schematically in Figure 3(b). The bottom cone is activated first to move the load downward, the experiment starts with the load in its lowest position, the top cone is activated to lift the mass upward for a period of T = 1.0 *s*, then the bottom cone activates and the top one becomes passive to sink the mass for the same period T. This cycle is repeated for 10 times to eliminate error. All sampling signals are collected by DAQ (National instruments, BNC-2111) and data is recorded by MATLAB (MathWorks).

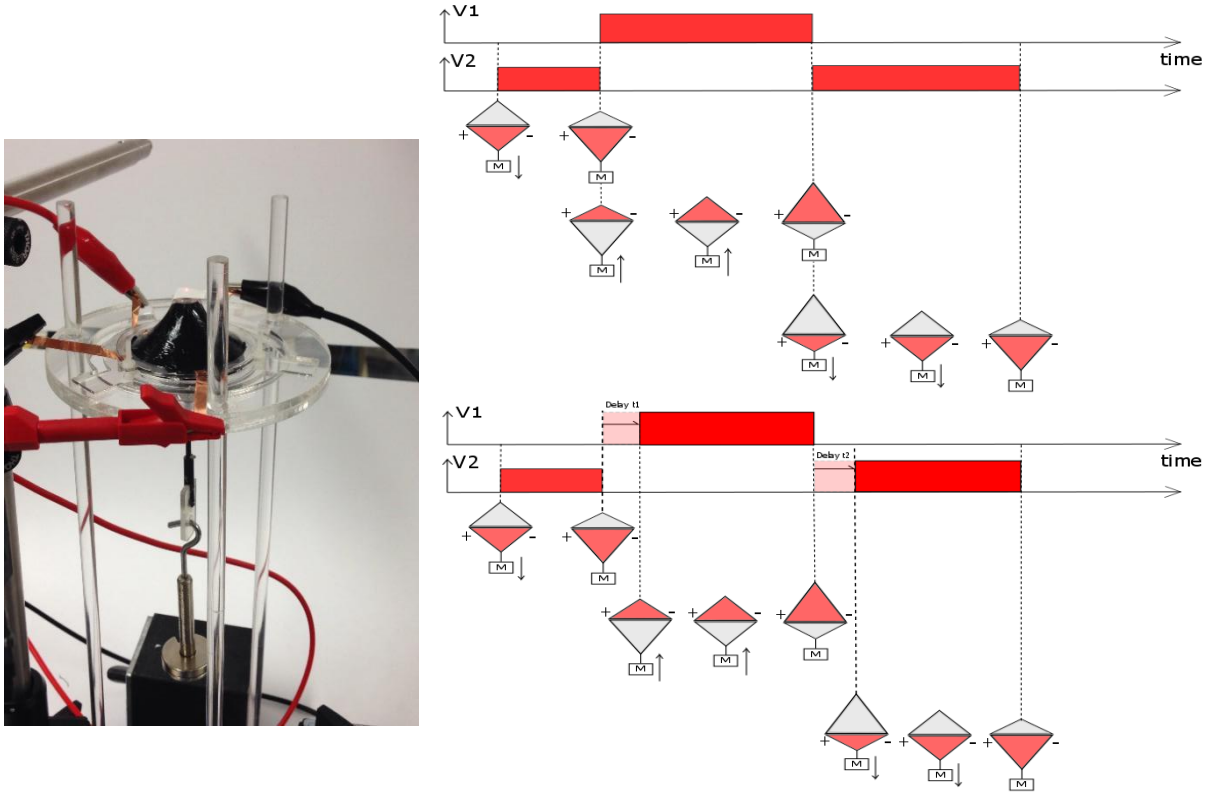

(a) (b)

Figure 3. (a). Energy analysis experiment setup, a double cone DEA is mounted on a testing rig, a 45 g mass is hanged at the bottom of the DEA. Two pairs of electrodes are connected to the DEA to drive the top and bottom cones separately. (b) Illustration of the actuation voltages of the DEA and the motions of the load and DEA end-effector. Top: two actuation voltages actuate without out delay; bottom: one actuation voltage is switched on with a delay time after the other voltage being switched off.

The actuation time of top and bottom cones is then reduced by t_1 and t_2 respectively thus to reduce the electrical energy input. This allows the load to move freely in the non-active period, and the concept is illustrated in Figure 3 (b). For simplicity, delay times t_1 and t_2 are set to be equal and increases from 0.0 s to 0.4 s, which accounts for 0 to 40% of the original actuation period T.

3.2 Leg prototype

A three-segment leg prototype was designed and fabricated, as is shown in Figure 4(a). All linkage bars are manufactured using fast prototyping techniques and 3 mm outer diameter miniature ball bearings are used in all joints to minimize frictional losses. The total weight of the leg is 21 g. The top of the leg is connected to a linear rail system in order to restrict the leg motion in a vertical direction. A rubber pad is placed underneath the foot to prevent the leg from slipping during actuation.

Figure 4 (b) shows the experiment setup, copper electrodes are connected to external high voltage cables which are hung to avoid adding any undesired load to the leg. The same alternating square driving voltage described in Section 3.1 was applied (amplitude: 3 kV, period: 1.0 s). No delay is introduced in this experiment.

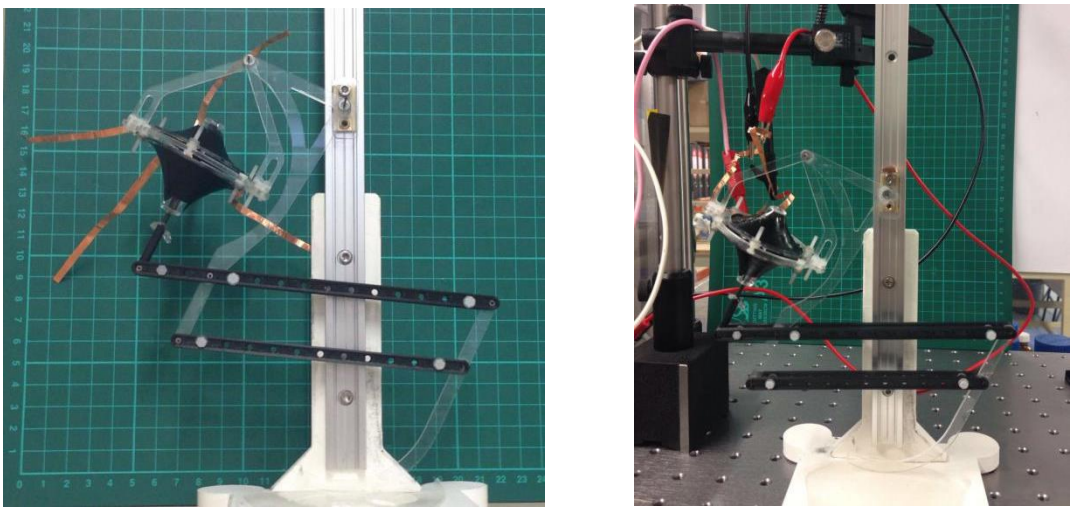

(a) (b)

Figure 4. (a) Three segment leg prototype with a linear slider. All linkages and the frames of DEA are either laser cut or 3D printed, ball bearings are used in all joints to reduce friction; (b) Leg motion experiment setup. Top and bottom cones are connected to two separate pairs of electrodes, all electrodes are hung on an external rig to avoid adding undesired mass to the leg.

4. RESULTS

4.1 Elastic energy recovery of DEA

The reaction force against displacement of the double cone DEA is shown in Figure 5. As shown, under the same displacement, stretching the DEA generates a slightly higher reaction force than recoiling, which is likely due to the Mullins effect. Both stretching and recoiling curves are approximately linear and thus in this work the reaction force and displacement relationship is estimated by a linear relationship of stiffness equal to 250 N/m.

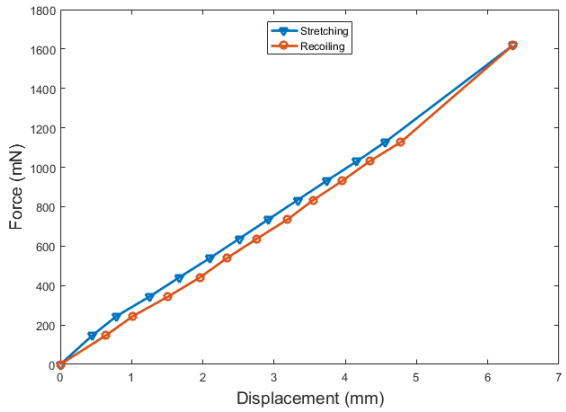

Figure 5. Elastic force on the DEA against displacement. Both stretching and recoiling curves are approximately linear, thus the elastic property of the DEA can be estimated as a linear spring with a stiffness of 250 N/m.

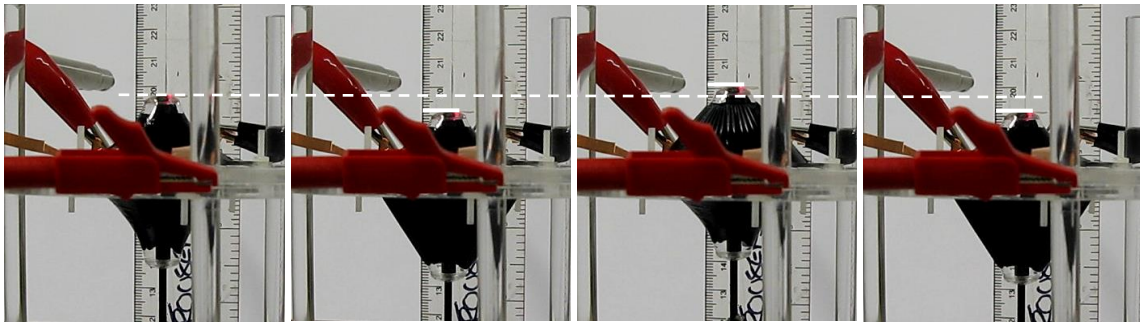

(a) (b) (c) (d)

Figure 6. Motion of the spacer (and load) when top and bottom cone DEAs are alternatively actuated. (a) to (d) shows the movement of the central spacer (also the load) under an alternating square driving voltages with an amplitude of 3 kV. Under 45 g load (~5 times the weight of actuator), the actuator is able to provide a stroke of 10.4 mm (4.8 mm upwards and 5.6 mm downwards), equaling to 23.6% of its height.

The stroke output of the DEA behaves differently with the delay time. For the no delay time case, the load moves at a relatively constant velocity from one terminal position to the other. At the end of each motion (travelling upwards or downward), its velocity reduces and finally reverses when the opposite actuator is switched on, as shown in Figure 7(a). However, in the case of a reduced actuation period, its motion has two more stages, as marked as (i) and (ii) in Figure 7(b). After the instant when one side of actuator is switched off, instead of moving towards the opposite side, the DEA spacer and the load continue moving in the same direction for a short period of time. This is likely due to the inertia of the load as well as any residual charge across the DEA electrodes. The load then reverses its heading and is driven by the passive elastic force exerted by the DEA (and its gravitational force if it moves downwards) until the opposite actuator is switched on after the delay time. Also it should be noted that DEA produces a greater stroke in the no delay time case than in the 0.4s delay case due to the longer actuation period.

Figure 7(c) and (d) compare the fluctuation of the elastic and gravitational potential energy in the system with 0.0s delay and 0.4s delay in driving voltage. Clearly more elastic and gravitational potential energy is stored and released in one cycle in the zero delay case. Kinetic energy is found to be in the magnitude of 10^{-6} mJ, thus can be safely neglected in this study. It should be noted that the net mechanical work done by the DEA in one complete cycle is zero since the load returns to its original position. Hence in the present study we focus only on the first half of the cycle when the gravitational load is raised upwards. Then the effective mechanical work W_{mech_eff} can be defined as

$$W_{mech\_eff} = E_{Gpotential}(t = T) - E_{Gpotential}(t = 0) \quad . \tag{5}$$

The efficiency of the system in the first half cycle can be defined as

$$\eta = \frac{W_{mech\_eff}}{E_{Eelectrical\_in}} \quad . \tag{6}$$

In the cases where actuation voltage is delayed by t_d, during the time period from $t = 0$ to $t = t_d$, gravitational potential energy in the load is gained only from the elastic potential energy in DEA, so we define the gained gravitational energy in this period as W_{rec} and is described as

$$W_{rec} = E_{Gpotential}(t = t_d) - E_{Gpotential}(t = 0) \quad . \tag{7}$$

It can be noticed from Figure 7(d) that only a part of the elastic potential energy stored in the DEA is recovered and is converted to the gravitational potential energy in the load work while the rest is lost. Here we introduce the elastic energy recovery factor as

$$\eta_{rec} = \frac{W_{rec}}{E_{elastic(t=t_d)} - E_{elastic(t=0)}} \quad . \tag{8}$$

Figure 8(a) compares the mechanical work done by the actuator, the energy recovered, the overall efficiency as well as the energy recovery factor from different delay time. The mechanical work output remains at its peak value and starts to drop after 0.14 s delay. On the other hand, the saved energy increases at short delay times (< ~0.16 s) then flattens and only accounts for a small proportion of the total mechanical work. The electromechanical efficiency fluctuates around 10% and has a small peak at t_d = 0.18s. A great increase can be seen in elastic energy recovery factor with the delay time. The electrical energy input in the first half of cycle is shown in Figure 8(b). Surprisingly, the energy inputs for the lowest delay time cases (< 0.16 s) are greater than that without delay, but the $E_{electical\_in}$ decreases with delay time after t_d = 0.04 s, which is as expected. Analysis of the unexpected inconsistencies with the electrical energy inputs has found that dynamics of the high voltage driver are inconsistent due to signal saturation under the higher electrical loading required for low and zero delay time cases causing. For example, the current over the last 0.5 s of the activation period (once a steady state value has been reached) increases from 5.851 µA for t_d = 0.0 s to 7.856 µA for t_d = 0.02 s and 8.711 µA for t_d = 0.04 s. For this reason, only measurements with time delays of 0.04 s and above are considered with respect to performance trends. Future work will investigate alternative high voltage driver circuits to eliminate their influence on the measure energy input values.

The experimental results suggest that for the forms of legged locomotion that do not require high power, such as walking, a large delay time can be chosen without losing much electromechanical efficiency and with the advantage of a greater proportion of elastic energy to be recovered. In contrast, when a large power output is required, no delay time or a low delay (e.g. t_d = 0.16 s) is suggested for the high power output and relatively low electrical energy input.

4. 2 Robot leg prototype

Driven by a single layer of double cone DEA, the robot leg is able to move downward by 10.1 mm and upwards by 7.8 mm, producing an overall stroke of 17.9 mm, which accounts for 9% of the leg's initial height. It should be noted that the leg design is not optimized and only a single layer DEA is applied here, so it is reasonable to believe that if all the leg parameters are optimized (e.g. leverage ratio a/b, as illustrated in Figure 9(a)) and multiple-layer DEAs are applied, better stroke output can be obtained.

5. CONCLUSIONS

The feature of having elastic energy recovery in DEAs enable this technology to have great potentials in legged locomotion, yet this feature has not been well studied and demonstrated in previous studies. In this work, by introducing a simplified DEA-mass system and adding delay into the DEA driving voltage, we were able to isolate and analyze the contribution of the elastic energy stored in DE membranes to the mechanical work output. Experimental results have shown that increasing the delay time in actuation voltage will increase the amount of elastic energy being recovered at first but this effect saturates. However, the elastic energy recovery factor increases monotonically with delay time. Increasing delay time reduces both mechanical work output and electrical energy input in general while leaving the electromechanical efficiency relatively constant. These results indicate that high delay time is more suitable for slower, more efficient walking locomotion gaits while full actuation period (no delay) is better for running or bouncing where high power output is desired. By applying the same DEA on a three-segment leg design, the leg was found to be able to move up and down by 17.9 mm (9% its initial height). With the feasibility of utilizing this double cone DEA on legs proven, in the future work we will optimize the leg design and analyze the elastic energy recovery on the DEA during driving the leg.

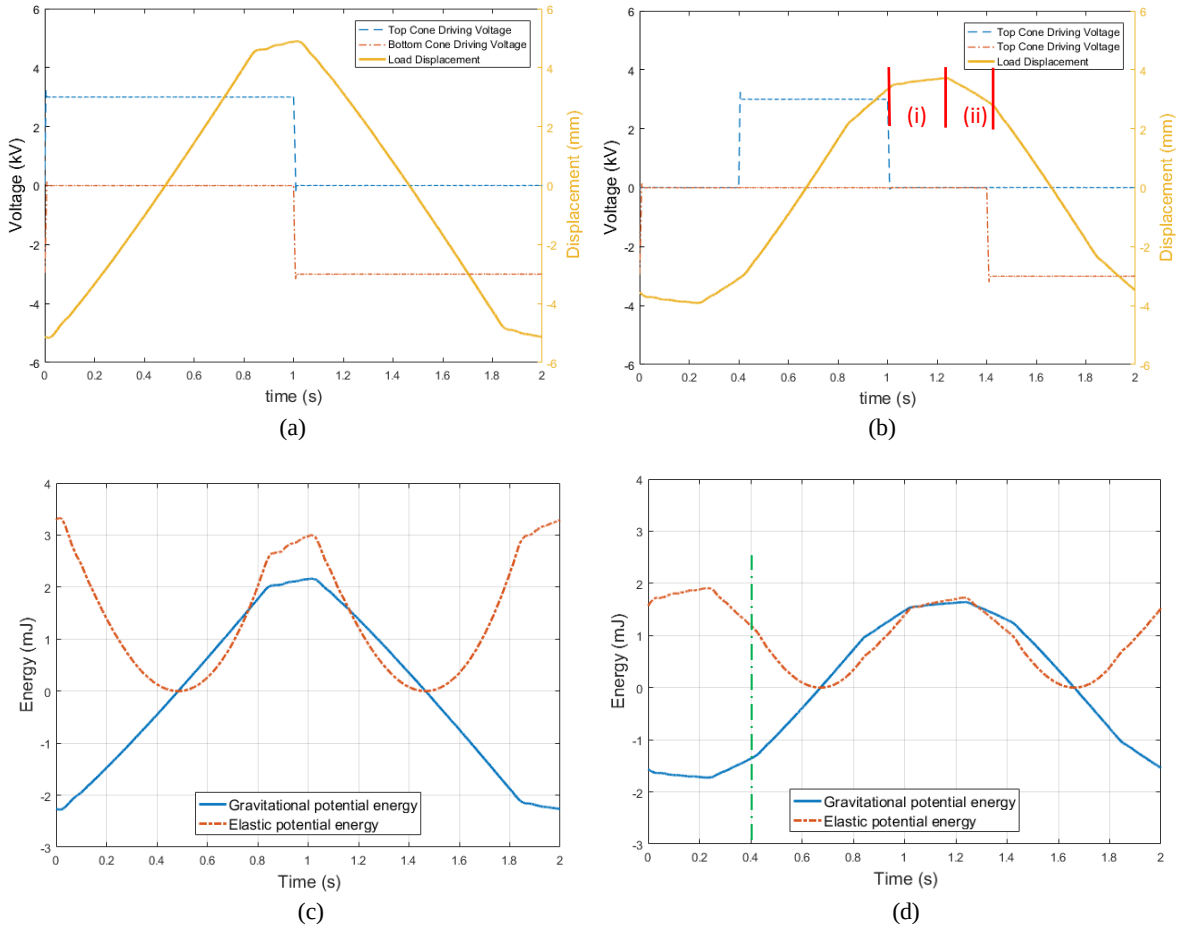

Figure 7. (a) Displacement of the load against time, t_d = 0.0 s; (b) Displacement of the load against time, t_d = 0.4 s; (c) Potential energy in the system against time, t_d = 0.0 s; (d) Potential energy in the system against time, t_d = 0.4 s.

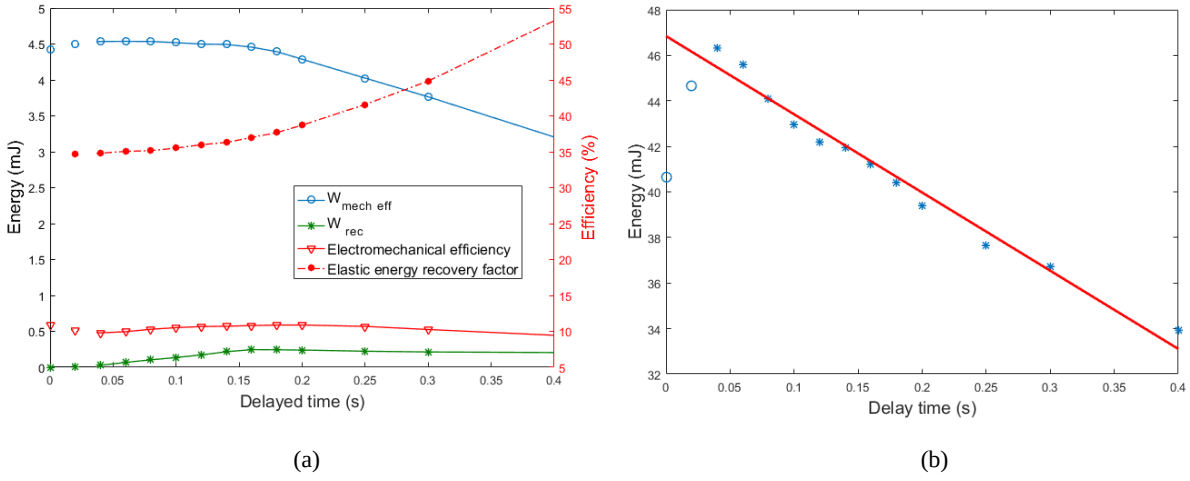

Figure 8. (a). Work output (mJ), energy recovery (mJ), electromechanical efficiency (%) and elastic energy recovery factor (%) against delay time; (b). Electrical energy input against delay time.

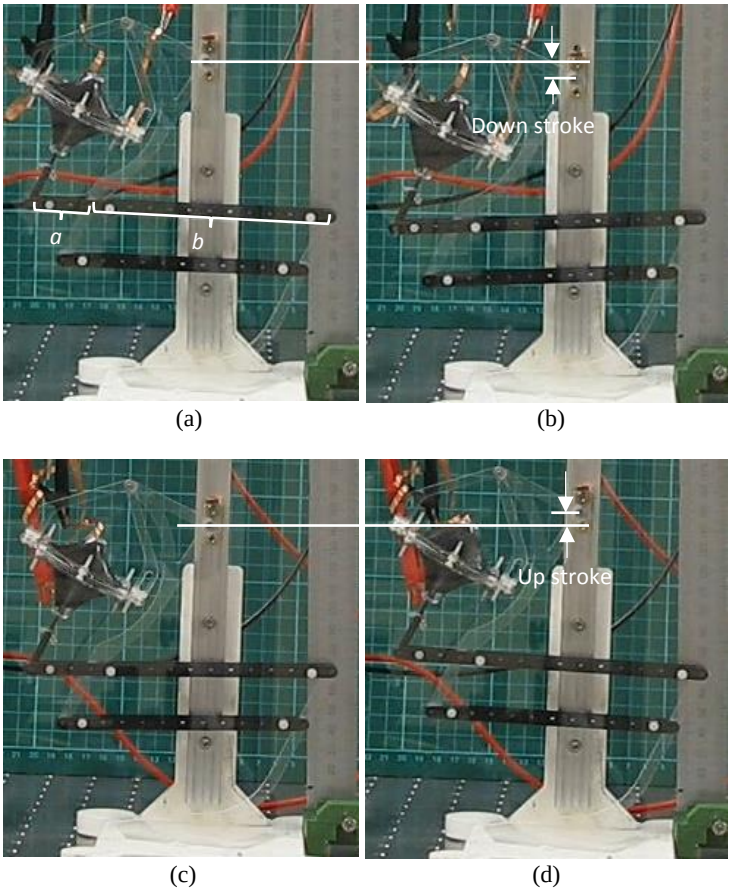

Figure 9. (a) Passive state; (b) Bottom cone is actuated, leg moves downward for 10.1 mm; (c) Passive state; (d) Top cone is actuated, leg moves upwards for 7.8 mm.

REFERENCES

[1] Carpi, F., Kornbluh, R., Sommer-Larsen, P. and Alici, G., "Electroactive polymer actuators as artificial muscles: are they ready for bioinspired applications?" Bioinspiration & biomimetics 6(4), 045006. (2011).

[2] Chouinard, P. and Plante, J.S., "Bistable antagonistic dielectric elastomer actuators for binary robotics and mechatronics" *IEEE/ASME Transactions on mechatronics 17*(5), pp.857-865. (2012).

[3] Wang, H. and Li, C., "A linear dielectric EAP actuator with large displacement output" In *2009 International Conference on Measuring Technology and Mechatronics Automation* (Vol. 1, pp. 73-76). IEEE. (2009).

[4] Pei, Q., Rosenthal, M., Stanford, S., Prahlad, H. and Pelrine, R., "Multiple-degrees-of-freedom electroelastomer roll actuators" Smart Materials and Structures 13(5), 86 (2004).

[5] Conn, A. T. and J. Rossiter., "Towards holonomic electro-elastomer actuators with six degrees of freedom." Smart Materials and Structures 3, 035012 (2012).

[6] Choi, H. R., Jung, K. M., Kwak, J. W., Lee, S. W., Kim, H. M., Jeon, J. H. and Nam, J. D., "Digital polymer motor for robotic application" *Proc. IEEE* International Conference on Robotics and Automation (ICRA) *2003*, 1857-62 (2003).

[7] Wang, P. and A. T. Conn., "Elastic Cube Actuator with Six Degrees of Freedom Output." Actuators 4(3), 203-216 (2015).

[8] Eckerle, J., Stanford, S., Marlow, J., Schmidt, R., Oh, S., Low, T. and Shastri, S. V., "Biologically inspired hexapedal robot using field-effect electroactive elastomer artificial muscles" In SPIE's 8th Annual International Symposium on Smart Structures and Materials., 269-280 (2001).

[9] Nguyen, C. T., Phung, H., Nguyen, T. D., Lee, C., Kim, U., Lee, D. and Choi, H. R., "A small biomimetic quadruped robot driven by multistacked dielectric elastomer actuators" Smart Materials and Structures. 23(6), 065005 (2014).

[10] Nguyen, C.T., Phung, H., Jung, H., Kim, U., Nguyen, T.D., Park, J., Moon, H., Koo, J.C. and Choi, H.R., "Printable monolithic hexapod robot driven by soft actuator" In: 2015 IEEE International Conference on Robotics and Automation (ICRA)., 4484-4489 (2015).

[11] Dubowsky, S., Kesner, S., Plante, J.S. and Boston, P., "Hopping mobility concept for search and rescue robots" Industrial Robot: An International Journal. 35(3), 238-245 (2008).

[12] Biewener, A. A., "Muscle-tendon stresses and elastic energy storage during locomotion in the horse" Comparative Biochemistry and Physiology Part B: Biochemistry and Molecular Biology. 120(1), 73-87 (1998).

[13] Hau, S., York, A. and Seelecke, S., "Performance prediction of circular dielectric electro-active polymers membrane actuators with various geometries". In *SPIE Smart Structures and Materials+ Nondestructive Evaluation and Health Monitoring.* International Society for Optics and Photonics., 94300 (2015).